Transportation Research Part C 76 (2017) 132–149

Contents lists available at ScienceDirect

Transportation Research Part C

journal homepage: www.elsevier.com/locate/trc

Fine-tuning ADAS algorithm parameters for optimizing traffic safety and mobility in connected vehicle environment

Hao Liu [a], Heng Wei [a,*], Ting Zuo [a], Zhixia Li [b], Y. Jeffrey Yang [c]

[a] Department of Civil and Architectural Engineering and Construction Management, College of Engineering and Applied Science, University of Cincinnati, 792 Rhodes Hall, Cincinnati, OH 45221-0071, USA
[b] Department of Civil and Environmental Engineering, WS Speed Hall 111, University of Louisville, Louisville, KY 40292, USA
[c] National Risk Management Research Laboratory, Water Supply and Water Resources Division, U.S. Environmental Protection Agency, Cincinnati, OH, USA

ARTICLE INFO

Article history:
Received 22 March 2016
Received in revised form 17 November 2016
Accepted 4 January 2017

Keywords:
Advanced Driver Assistance System (ADAS)
Driver behavior modeling
Microscopic traffic flow modeling
Traffic safety and mobility optimization

ABSTRACT

Under the Connected Vehicle environment where vehicles and road-side infrastructure can communicate wirelessly, the Advanced Driver Assistance Systems (ADAS) can be adopted as an actuator for achieving traffic safety and mobility optimization at highway facilities. In this regard, the traffic management centers need to identify the optimal ADAS algorithm parameter set that leads to the optimization of the traffic safety and mobility performance, and broadcast the optimal parameter set wirelessly to individual ADAS-equipped vehicles. Once the ADAS-equipped drivers implement the optimal parameter set, they become active agents that work cooperatively to prevent traffic conflicts, and suppress the development of traffic oscillations into heavy traffic jams. Measuring systematic effectiveness of this traffic management requires am analytic capability to capture the quantified impact of the ADAS on individual drivers' behaviors and the aggregated traffic safety and mobility improvement due to such an impact. To this end, this research proposes a synthetic methodology that incorporates the ADAS-affected driving behavior modeling and state-of-the-art microscopic traffic flow modeling into a virtually simulated environment. Building on such an environment, the optimal ADAS algorithm parameter set is identified through a multi-objective optimization approach that uses the Genetic Algorithm. The developed methodology is tested at a freeway facility under low, medium and high ADAS market penetration rate scenarios. The case study reveals that fine-tuning the ADAS algorithm parameter can significantly improve the throughput and reduce the traffic delay and conflicts at the study site in the medium and high penetration scenarios. In these scenarios, the ADAS algorithm parameter optimization is necessary. Otherwise the ADAS will intensify the behavior heterogeneity among drivers, resulting in little traffic safety improvement and negative mobility impact. In the high penetration rate scenario, the identified optimal ADAS algorithm parameter set can be used to support different control objectives (e.g., safety improvement has priority vs. mobility improvement has priority).

* Corresponding author.
E-mail address: heng.wei@uc.edu (H. Wei).

http://dx.doi.org/10.1016/j.trc.2017.01.003
0968-090X/

1. Introduction

The Advanced Driver Assistance Systems (ADAS) have been widely accepted in the last decade as an effective technology for assisting drivers to avoid traffic accidents (NHTSA, 2015; Bengler et al., 2014). One of the core components of the ADAS is the alarm algorithms (Ararat et al., 2006; ISO 15623, 2002; Kiefer et al., 2003; Brunson et al., 2002). The algorithms define multiple criteria that specify the maximum speed a driver is allowed to drive at a road segment, the minimum following headway or spacing the driver should maintain, the safe gap for lane changes, and the timing at which the driver should take evasive actions to avoid a collision (Adell et al., 2011; Nodine et al., 2011; Farah et al., 2012; Birrell et al., 2014; Várhelyi et al., 2015). If any of the criteria is violated, the ADAS will warn the driver via video, audio or haptic messages (Farah and Koutsopoulos, 2014), or even directly intervene the driving task in critical situations (Coelingh et al., 2010). Because of the features, the ADAS is able to effectively reshape the drivers' behaviors such that they will interact more properly and quickly with the traffic environment (Birrell et al., 2014), and their maneuvers more harmonious in a traffic stream (Farah et al., 2012). Subsequently, many traffic conflicts (near miss traffic accidents) can be avoided and the associated traffic disturbances dampened. As a result, the operation of a traffic stream would be greatly improved with enhanced safety.

With the advancement of the Connected Vehicle (CV) technology that enables wireless communication among vehicles and road-side infrastructure (Jones, 2013; Shladover et al., 2012; Kesting et al., 2010), the ADAS's capability of improving traffic safety and mobility can be further amplified through the collaborative efforts of the traffic management centers and the ADAS users. To this end, the traffic management centers first perform scenario-based analyses for a concerned highway facility based on the real-time or projected traffic conditions (e.g., traffic demand and fleet composition), the ADAS marketing penetration rate (i.e., the percentage of vehicles that are equipped with the ADAS), and the drivers' acceptance or compliance level to the ADAS assistance. In these analyses, the ADAS with various algorithm parameter levels are assumed to be deployed consistently in the vehicle fleet. The output of the analyses is a specific set of the ADAS algorithm parameters that enables the maximum safety and mobility improvement of the concerned facility. Such an ADAS algorithm parameter set is referred to as the optimal ADAS algorithm parameter set. The optimal ADAS algorithm parameter set is then broadcasted via the wireless communication to individual ADAS-equipped vehicles. Once the ADAS-equipped drivers implement the optimal parameter set, they become active agents that work cooperatively to prevent traffic conflicts, and suppress the development of traffic oscillations into heavy traffic jams.

To identify the optimal ADAS parameter set, we need to quantify the impact of the ADAS on individual drivers' behaviors, and estimate the systematic safety and mobility improvement due to the behavior impact. The existing ADAS effectiveness studies, however, mainly adopt field or simulator-based evaluation methods that can test the behavior adaptation for a small group of test drivers (Bueno et al., 2014; Várhelyi et al., 2015). It is not technically or economically feasible to identify the systematic impact of the ADAS within the existing evaluation framework. To address this challenge, a cost-effective no-risky synthetic approach is developed in this study to capture the effectiveness of the ADAS on individual drivers' driving behaviors, and the subsequent aggregated influence of such affected behaviors impacts on traffic mobility and safety from a systematic standpoint of the CV-involved traffic flows. This integrated methodology is built into a microscopic simulation environment to investigate how the ADAS equipped within individual vehicles can be implemented cooperatively to optimize the traffic flow operation. Specifically, we first establish the functional relationship between the ADAS algorithm parameters and the drivers' behavior adaptation based on findings of the existing ADAS effectiveness studies. The identified ADAS-affected behavior parameters are then embedded into the state of the art microscopic traffic flow models as factors representing drivers' response sensitivity to traffic stimuli, such as relative speed and spacing between the subject driver and the leading vehicle. The traffic flow models are used to realistically reproduce the vehicle activity data, which provides the basis for computing the safety and mobility measures of effectiveness (MOEs). Finally, a multi-objective optimization framework that employs the Genetic Algorithm (Miettinen, 2012) is adopted to iteratively execute the simulation model until it identifies the optimal ADAS algorithm parameter set that maximize the MOEs.

The paper is organized as follows. In Section 2, a comprehensive literature review is conducted to summarize the major functionality of the ADAS, the ADAS-affected driving behaviors, and the systematic impact of the ADAS on traffic safety, mobility and emission reduction. Section 3 discusses the methodology framework of the presented research. In Section 3.1, the alarm algorithm of a major ADAS function (i.e., forward collision warning) is elaborated and the key parameters of the algorithm are identified. Section 3.2 contains the modeling methods of the ADAS-affected behaviors, and the incorporation of the ADAS-affected behaviors into the microscopic traffic flow models. Section 3.3 describes the multi-objective optimization method used for searching for the optimal ADAS algorithm parameter set. In Section 4, the presented methodology is tested in a case study performed at a realistic freeway site. Finally, the conclusion of the research is presented in Section 5.

2. Literature review

A typical ADAS can provide user assistance functions including forward collision warning (FCW), speed limit warning (SLW), curve speed warning (CSW), lane departure warning (LDW), and/or blind spot warning (BSW). Among them, the FCW, SLW and CSW are designed to assist the longitudinal movement of subject drivers, whereas the LDW and BSW for the lateral movement. In the remaining sections of the paper, the FCW, SLW and CSW are referred to as the longitudinal movement assistance functions and the LDW and BSW are referred to as the lateral movement assistance functions. The

impact of these functions on driving behaviors is summarized in Tables 1 and 2. Table 1 includes field tests of the ADAS; whereas Table 2 contains the simulator based studies. The Cooperative Adaptive Cruise Control (CACC) is also a widely studied ADAS function. Nonetheless, the CACC automatically performs longitudinal vehicle control, rather than affects drivers' behaviors.

Table 1
Field tests of ADAS regarding its impact on driving behaviors.

Study	Study Description	System Impact on Behaviors
Ben-Yaacov et al. (2002)	Field tests of FCW effect tiveness. Alarmed sounded if headway less than 1 s	**Headway (HW, in sec)** % of time HW in 0–0.4 s, Base/FCW: 9%/0%; % of time in 0.4–0.8 s, Base/FCW: 34%/2%; % of time in 0.8–1.2 s, Base/FCW: 17%/20%; % of time in 1.2–1.6 s, Base/FCW: 5%/22%; % of time in 1.6-2 s, Base/FCW: 3%/7%
Shinar and Schechtman (2002)	Field tests of FCW effectiveness. Initial warning if HW < 2.5 s; red light warning if HW < 1.2 s; and red light plus audio warning if HW < 0.8 s	**HW (s)** % of time HW < 0.8 s, Base/FCW: 20.1%/14.6%; % of time HW in 0.8–1.2 s, Base/FCW: 22.8%/20.9%; % of time HW > 1.2 s, Base/FCW: 57.1%/64.5%
Adell et al. (2011)	Field tests of an ADAS named the SASPENCE system, developed in the EU-financed project PReVENT. Alarm sounded when following too close, there is a risk of rear-end collision, high speed when entering curve road, and speed over the speed limit	**PRT (Perception-Reaction Time, in sec) in case of curve alarms** Freeway, Base/ADAS: 4.7/2.6 Urban, Base/ADAS: 3.8/1.8 Rural, Base/ADAS: 3.1/2.7 **PRT in case of obstacle alarms**Freeway, Base/ADAS: 4.1/3.2 Urban, Base/ADAS: 3.0/2.6 Rural, Base/ADAS: 3.7/3.2 **User Trust (0–100)** Safe Distance Function: 83 Safe Speed Function: 77 Speed Limit Warning: 88
Nodine et al. (2011)	Field tests of an ADAS named the Integrated Vehicle-Based Safety System (IVBSS). The system provides FCW, CSW, BSW, and LDW. A TTC-based algorithm is adopted to determine the FCW warnings	**PRT (s)** Base/IVBSS: 1.03/0.58 **Speed (m/s)** Base/IVBSS: 24.7/24.9 **HW (s)** Freeway Base/IVBSS: 1.41/1.37 Freeway Base/IVBSS: 2.05/1.98 **Number of Lane Changes per 100 Miles Driven** Freeway Base/IVBSS: 49.1/48.8 Freeway Base/IVBSS: 38.2/36.5 **Perceived Usefulness (0–100)** Male/Female: 51/55
Farah et al. (2012)	Field tests of an ADAS named the CO-OPerative SystEms for Intelligent Road Safety (COOPERS). COOPERS provides speed limit advice, SLW, accident/road work/congestion warning, weather warning, and LDW	**Speed (km/h)** Base/ COOPERS: 101.60/100.01 (speed limit 100 km/h) **HW (s)** Base/COOPERS: 1.52/1.55 **User Acceptance (0–7)** System useful: 6 Improve prompt maneuver: 5.6 Improve safety: 5.5
Birrell et al. (2014)	Field tests of a smartphone-based ADAS that was developed by the U.K. project Foot-LITE. Yellow warning sounded if HW < 2 s and red warning if HW < 1.5 s. It also contains LDW, gear change advice, acceleration and braking advice	**HW (s)** Base/ADAS: 2.05/2.33 Base/ADAS in HW < 1.5 s: 6.61%/2.32%
Farah and Koutsopoulos (2014)	Field tests of an ADAS named the CO-OPerative SystEms for Intelligent Road Safety (COOPERS). COOPERS provides speed limit advice, SLW, accident/road work/congestion warning, weather warning, and LDW	Measured data used to compute parameters in the GHR model. Parameters are driver age dependent
Várhelyi et al. (2015)	Field tests of an ADAS named the Continuous Support (CS), which is developed in the EU-financed interactIVe project. It provides FCW, SLW, CSW and BSW	Improvement in speed in curves, speed adaptation and side collision reduction Deterioration in speed when turning, dangerous distance to the side

Table 2
Simulator tests of ADAS regarding its impact on driving behaviors.

Study	Study description	System impact on behaviors
Lee et al. (2002)	Simulator-based tests of FCW effectiveness. Kinematic algorithm adopted in the FCW for determining behavior thresholds. Assumed follower deceleration 0.40 g for early warning (EW) and 0.75 g for late warning (LW). Initial speed 56.3/88.5 km/h. Lead vehicle deceleration 0.40/0.55 g. Initial headway 1.70/2.50 s	**PRT (s)** Distracted drivers, Base/EW/LW: 2.21/1.35/2.10 Non-districted drivers, Base/EW: 1.30/0.70
McGehee et al. (2002)	Simulator-based tests of FCW effectiveness. Kinematic algorithm adopted in the FCW. Assumed follower deceleration 0.75 g. Assumed subject driver PRT 1.0 s for late warning (LW) and 1.5 s for early warning (EW). Lead vehicle stops	**PRT (s)** EW, Base/FCW: 2.53/1.93 LW, Base/FCW: 2.53/2.23
Mulder et al. (2004)	Simulator-based tests of FCW effectiveness. Subject drivers are asked to maintain an HW of 1.5 s and perform secondary tasks. The FCW provides gas pedal haptic feedback computed based on HW and TTC. Two feedback types: force feedback (FF) that relies on HW and TTC and stiffness feedback (SF) that relies on HW only	**Standard deviation of HW (s)** Base/FF/SF: 0.228/0.203/0.205 **Median HW (s)** Base/FF/SF: 1.52/1.58/1.66 **Mean PRT (s), central visual stimuli** Base/FF/SF: 0.511/0.525/0.488 **Mean PRT (s), peripheral visual stimuli** Base/FF/SF: 0.503/0.524/0.492
Abe and Richardson (2006)	Simulator-based tests of FCW effectiveness. Stop-Distance-Algorithm adopted in the FCW. Assumed follower deceleration 0.45 g for early warning (EW) and 0.60 g for late warning (LW). Initial speed 40/60/70 mph. Initial headway 1.70/2.20 s (SHW/LHW). Lead vehicle deceleration 0.8 g	**PRT (s)** EW, SHW, mean Base/FCW: 0.82/0.60 EW, SHW, std Base/FCW: 0.5/0.15 EW, LHW, mean Base/FCW: 0.81/0.81 EW, LHW, std Base/FCW: 0.5/0.3 LW, SHW, mean Base/FCW: 0.65/0.65 LW, LHW, std Base/FCW: 0.2/0.4 **User Trust (Grade 0–10)** SHW, EW/LW: 6.7/5.2 LHW, EW/LW: 6.8/3.9
Jamson et al. (2008)	Simulator-based tests of FCW effectiveness. Adaptive and non-adaptive FCW tested. Adaptive FCW (AFCW) captures the subject driver's PRT. Warning based on Stop-Distance-Algorithm. Initial HW = 1 s and speed = 50 mph. Lead vehicle brakes in 4 m/s^2 until reaching 5 mph, continuing the speed for 10 s and then accelerating back to 50 mph	**PRT (s)** Expected events, Base/FCW/AFCW: 1.1/1.2/1.1 Unexpected events, Base/FCW/AFCW: 6.1/5.2/4.9 **User Trust (0–100)** FCW/AFCW: 62/63
Mohebbi et al. (2009)	Simulator-based tests of FCW effectiveness. Warning based on a threshold TTC of 5 s. Tactile warning (TW) or audio warning (AW) provided. Initial HW = 2 s and speed between 55 and 65 mph. Leader brakes in 6 m/s^2 until stop. Subject drivers engage in hands-free cell phone conversations	**PRT (s)** None conversation, Base/TW/AW: 0.76/0.67/0.69 Simple conversation, Base/TW/AW: 0.93/0.73/0.85 Complex conversation, Base/TW/AW: 0.96/0.83/0.90
Koustanaï et al. (2012)	Simulator-based tests of FCW effectiveness. Stop-Distance-Algorithm adopted in the FCW. Initial speed = 90 km/h. Lead vehicle brakes in 3.0 m/s^2 (braking scenario, BS) or 5.0 m/s^2 (emergency braking scenario, ES). The test drivers may be familiar with the FCW (familiar group, FG) or not familiar with the system (unfamiliar group, UG). Drivers asked to perform secondary tasks	**PRT (s)** ES, Base/UG/FG: 3.4/1.5/1.4 BS, Base/UG/FG: 3.0/1.8/1.7 **HW (s)** ES, Base/UG/FG: 3.2/3.6/5.8 BS, Base/UG/FG: 4.6/5.0/5.4 **User Trust (0–10)** UG: 5.3 FG: 6.3
Aust et al. (2013)	Simulator-based tests of FCW effectiveness. Alarm issued based on a spacing algorithm. Initial speed 90–100 km/h, initial HW = 1.5 s (SHW) or 2.5 s (LHW). Lead vehicle brakes in 0.55 g. Each test driver encountered 6 braking events (E1-E6)	**PRT (s)** SHW, Base/FCW: E1, 2.25/2.14; E3, 1.91/1.10; E5, 1.87/1.18 LHW, Base/FCW: E1, 3.10/2.87; E3, 2.76/1.37; E5, 2.46/1.19
Bueno et al. (2014)	Simulator-based tests of FCW effectiveness. Stop-Distance-Algorithm adopted in the FCW. Initial HW = 2 s and initial speed = 90 km/h. Lead vehicle brakes for 2.5 s to reach 0.8 s HW. Subject drivers perform distraction secondary tasks (DT)	**PRT Reduction (s)** Light DT Group: 0.15 s before DT; 0.07 s during DT; and 0.12 s after DT Heavy DT Group: 0.12 s before DT; 0.02 s during DT; and 0.07 s after DT **Mental Demand** Test drivers report less mental demand with the assistance of the FCW

Above tables indicate that the simulator-based study is often used in the early stage of the ADAS development; whereas the field tests are mostly conducted as the technologies become more mature. The simulator-based tests usually focus on exploring the effectiveness of specific ADAS functionalities or improving the design of the ADAS algorithms. On the other hand, the field tests mainly concern the reliability of the entire ADAS system. In this case, the tests not only monitor the behavior impact, but also examine system aspects such as the reliability of the wireless communication and the human interface design. The majority of driver behaviors tested in the studies have two common features: (1) they are correlated with the traffic safety performance; and (2) they can be quantitatively measured by using existing sensing technologies. Besides these tested behavior parameters, some less studied ADAS-affected behaviors might also have significant impact on the traffic flow operation. Examples include the variation of a ADAS-equipped driver's behavior adaptation under different traffic conditions and driver mental states, the behavior patterns of the driver after using the ADAS for a long period of time, and the behavior adaptation of non-equipped drivers as they interact with the ADAS-equipped drivers. Since these parameters are difficult to measure with the existing methods, the development of more sophisticated experimental design and more advanced measuring technologies is required to address the challenge. In addition, the functionality description of the ADAS indicates that the ADAS might also affect behaviors related to the traffic flow stability. Such behaviors include the drivers' short-term prediction of surrounding vehicles' speed and location, and the multi-anticipation behavior that takes into account multiple leading vehicles in the car-following state. Unfortunately, these behaviors are not considered by the listed studies. Such a research limitation requires attention of the future studies.

Tables 1 and 2 indicate that the FCW is the most tested function of the ADAS. It has potential to affect subject drivers' perception-reaction time and desired following headways. As the FCW is expected to be widely adopted by users in the near future, this function and its affected behaviors are selected in this study to demonstrate the methodology for ADAS algorithm parameter optimization.

The effectiveness of the ADAS is usually evaluated by the simulation studies. A summary of the studies is provided in Table 3. It reveals that a great research effort has been made to estimate the safety, mobility and environmental impact of systems that automatically perform driving tasks for drivers (e.g., CACC). A relatively fewer studies concern the driver assistance functionalities of the ADAS, due to the lack of the analysis capability for capturing the ADAS-equipped drivers' behavior adaptation. The studies that do explore the effectiveness of the driver assistance functionalities (e.g., Lundgren and Tapani, 2006; Khondaker and Kattan, 2015) fail to model the behavior adaptation as a function as the ADAS control algorithms. The test results from studies listed in Tables 1 and 2 are not fully exploited to quantify the range of the behavior adaptation or explore the functional relationship between ADAS-equipped drivers' behavior adaptation and the ADAS algorithm parameters. Without the consideration, their methodologies are not able to consider the duration and intensity of

Table 3
Systematic impact of ADAS on traffic flow operation.

Study	System analyzed	Behavior considered	Traffic flow models	System impact
Lundgren and Tapani (2006)	ADAS (no function specified)	PRT (0–1.5 s) and desired headway (1–3 s)	Gazis-Herman-Rothery (GHR) model for car-following (CF) behavior	130% increase of time-exposed time-to-collision (TET) and 280% increase of time-integrated TTC (TIT) as PRT increases from 0 to 1.5 s; 233% decrease of TET and 300% decrease of TIT as desired headway increases from 1 to 3 s
Van Arem et al. (2006)	CACC	NA	The MIXIC model for CF and lane-changing (LC) behavior	Reduction in number of shockwaves and increase in average speed as CACC penetration rates increases. Reduction in traffic safety because CACC vehicle platoons prevent other vehicles from merging. No significant impact on throughput
Hegeman et al. (2009)	Overtaking assistant system (OAS)	Driver's overtaking frequency	The rural traffic simulator (RuTSim)	The impact of OAS penetration rate was not significant. The 11 s minimum overtaking time threshold was found to minimize the safety measures such as minimum time-to-collision (TTC), TET and TIT
Schakel et al. (2010)	CACC and acceleration advice controller (ACC)	Driver's acceleration affected by ACC	Intelligent Driver Model (IDM) for CF behavior	Traffic stability is analyzed for a single lane road with 2000 veh/h traffic load. The non-CV case has growing shockwave duration and range. The AAC and CACC cases have decreased shockwave duration and increase shockwave range and speed
Kesting et al. (2010)	Adaptive cruise control (ACC).	NA	IDM and constant-acceleration heuristic	0.3% increase of maximum flow rate due to 1% increase of ACC penetration rate
Wang et al. (2014)	Ecological adaptive cruise control (EcoACC)	NA	The EcoACC control inputs determined based on model predictive control	With EcoACC, 17% reduction in flow and vehicle mile traveled (VMT) and 19.5% reduction in average CO2 emission under low density traffic (20 veh/km); 31.3% increase in flow and VMT and 9% reduction in average CO_2 emission under high density traffic (40 veh/km)
Khondaker and Kattan (2015)	Variable Speed Limit (VSL) under the CV environment	Desired speed	IDM for CF behavior	20% reduction of total travel time, 6–11% of safety improvement, and 5–16% reduction in fuel consumption under 100% CV penetration rate

ADAS's impact on individual driver, or the randomness of the level of impact on different drivers. Hence the outputs of these methodologies might be incapable of accurately reflecting the systematic impact of the ADAS.

3. Methodology

The following table lists the notations used in the presented research (see Table 4).

The methodology framework for identifying the optimal ADAS algorithm parameter set is illustrated by Fig. 1. The framework elaborates major components involved in this research, and governing equations adopted by individual component. Numbers in the shaded circles represent subsections that discuss the corresponding components. In this study, we focus on the modeling of the perception-reaction time (PRT) and desired headway (DH) adaptation, because these parameters can be significantly affected by the FCW (see Sections 3.1 and 3.2). When looking for the optimal ADAS parameter set, we do not apply an explicit objective function that quantify the relationship between the ADAS parameter and the MOEs. Instead, the functional relationship is obtained implicitly through executing the presented traffic flow models (see Section 3.3). A major assumption in this study is that a driver makes behavior changes only when the ADAS is interacting with the driver. If the ADAS does not provide warning or advisory information, the driver is assumed to behave similarly to the non-ADAS equipped drivers. In this case, the ADAS-equipped drivers' long-term behavior adaptation is not considered.

3.1. Identification of target ADAS algorithm parameters

As one of the most important functions in ADAS, the FCW is considered in the presented study. The FCW function determines the driving behavior criteria based on the kinematic and perceptual approach (Bella and Russo, 2011). With the perceptual approach, an alarm is triggered once the subject driver's headway or time-to-collision (TTC) to the leading vehicle is lower than the pre-specified critical headway or TTC threshold (Shinar and Schechtman, 2002; Mulder et al., 2004; Mohebbi et al., 2009). On the other hand, the kinematic approach continuously compares the subject driver's following distance (or spacing) with the warning distance, which is a function of the host vehicle's speed, the relative speed and spacing between

Table 4
Notations used in the research.

ADAS Algorithm	
HW_{ADAS} (s)	Threshold headway used by the ADAS algorithm. It represents the smallest safe headway. HW^{*}_{ADAS} represents the boundary of the threshold headway
WD (m)	Warning distance, a threshold distance used by the ADAS algorithm. It represents the shortest safe spacing between a subject vehicle and its leading vehicle
H	Subject vehicle that hosts the ADAS system
L	Leading vehicle in front of the subject vehicle
A_{Hmax} (m/s^2)	Anticipated maximum deceleration of the subject driver
A (m/s^2)	Current acceleration
V (m/s)	Current speed
T_{LS} (s)	Time for the leading vehicle to stop: $T_{LS} = -V_L/A_L$
T_{FS} (s)	Time for the subject vehicle to stop: $T_{HS} = T - (V_H + A_H \cdot PRT)/A_{Hmax}$ if $V_H + A_H \cdot PRT > 0$, or $T_{HS} = -V_H/A_H$
RR (m/s)	Range rate, which equals to $V_L - V_H$
D_0 (m)	Minimum distance between the leading vehicle and the host vehicle
T_M (s)	Time when RR is 0: $T_M = \{[RR + (A_L - A_H)PRT]/(A_{Hmax} - A_L)\} + PRT$ if $T_M > PRT$, otherwise $T_M = PRT$
WD^{*}_{ADAS} (m)	Boundary of the warning distance, a function of the WD
Driver behavior parameters	
σ	Compliance level, a random number with a range of 0–100
DH^{*} (s)	Desired headway affected by the ADAS
PRT^{*} (s)	Perception-reaction time affected by the ADAS
DH_0 (s)	Desired headway of a driver not equipped with the ADAS
PRT_0 (s)	Perception-reaction time of a driver not equipped with the ADAS
Δt_1 (s)	ADAS influence time
Δt_2 (s)	Recovering time
Car-following and lane-changing models	
$\dot{v}$ (m/s^2)	Acceleration of a modeled vehicle
a (m/s^2)	Maximum (acceptable) acceleration of a modeled driver
b (m/s^2)	Maximum (acceptable) deceleration of a modeled driver
v_0 (m/s)	Desired speed of a modeled driver
v (m/s)	Actual speed of a modeled driver
Δv (m/s)	Relative speed with the leading driver
s^{*} (m)	Desired following spacing
s_0 (m)	Spacing in jam traffic
s (m)	Actual spacing between a subject driver and the leading driver
α, β	Model coefficients in the intelligent driver model

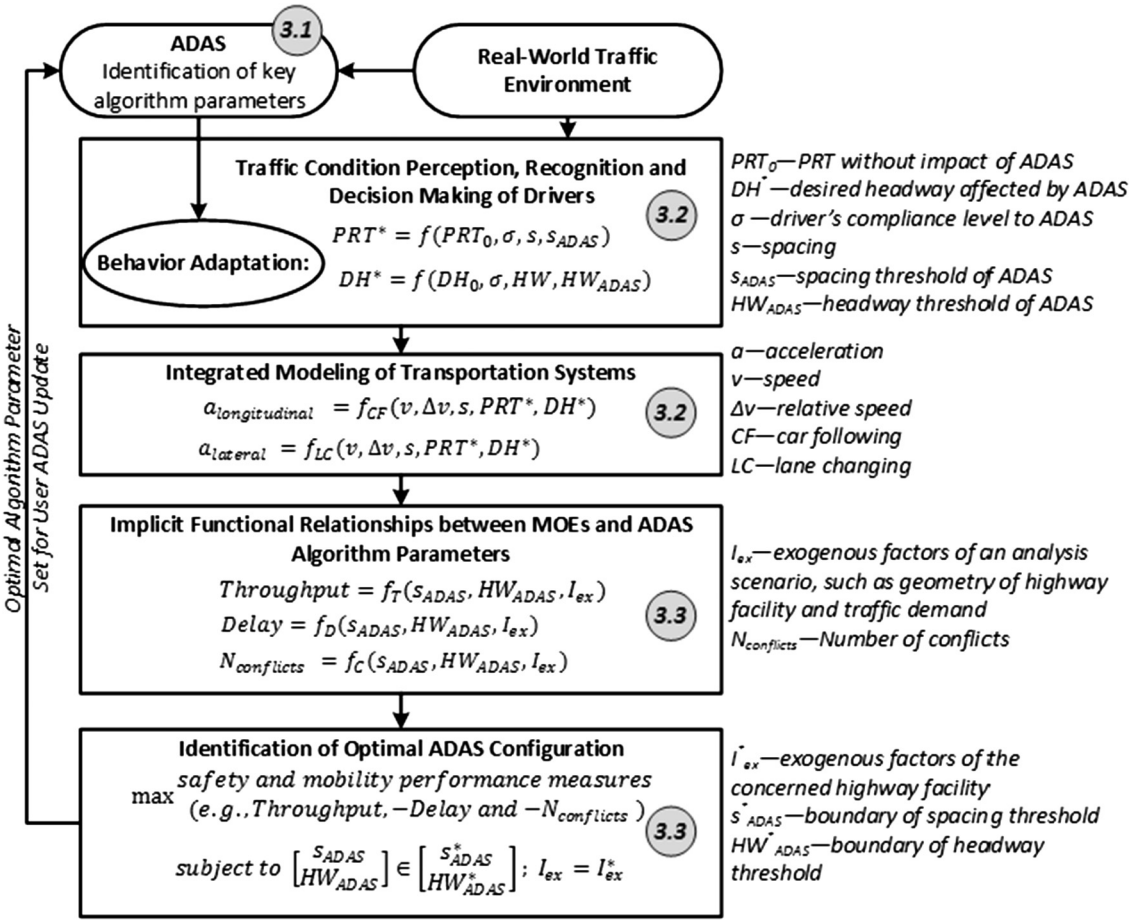

Fig. 1. Methodology framework for identifying optimal ADAS configuration.

the host vehicle and the leading vehicle. If the spacing is shorter than the warning distance, the ADAS will issue a warning message to the subject driver (Brunson et al., 2002).

In some studies, the perceptual approaches that adopt the TTC based thresholds are reported (Mulder et al., 2004; Mohebbi et al., 2009; Nodine et al., 2011), and in other studies the headway based thresholds are applied (Shinar and Schechtman, 2002; Birrell et al., 2014). The TTC or headway threshold of an ADAS is usually directly set to a fixed value. The reported TTC thresholds range from 2.0 s to 5.0 s, whereas the headway thresholds are between 1.2 s to 2.4 s. Both TTC thresholds and headway thresholds can be adopted to affect the subject driver's desired car-following distance. In this study, the headway threshold is selected as an ADAS algorithm parameter to be optimized later, because it can be directly associated with the subject driver's car-following behavior. The boundary of the headway threshold is given as:

$$HW^*_{ADAS} \in [1.2s, 2.4s] \tag{1}$$

Above boundary specifies the field within which the search for the optimal headway threshold should be performed.

The kinematic approach adopts algorithms such as the Mazda algorithm (Ararat et al., 2006), the stopping distance algorithm (ISO 15623, 2002), the CAMP algorithm (Kiefer et al., 2003), and the National Highway Traffic Safety Administration (NHTSA) algorithm (Brunson et al., 2002). In this study, the NHTSA algorithm is adopted because it considers different cases as the host vehicle approaches the leading vehicle in a potential collision course. Specific model formulations are applied for computing the warning distance in individual cases. Particularly, when an initially moving leading vehicle stops prior to the host vehicle or the leading vehicle is initially stopped, the following condition should be met:

$$T_{LS} < T_{FS} \tag{2}$$

The warning distance is:

$$WD = 0.5(A_{Hmax} - A_H)PRT^2 + 0.5A_L T_{LS}^2 + (A_H - A_{Hmax})PRT \cdot T_{HS} - RR \cdot T_{HS} - A_L T_{HS} T_{LS} + 0.5A_{Hmax}(T_{HS})^2 + D_0 \tag{3}$$

When the host vehicle stops while the leading vehicle is still in motion or $T_{LS} \geqslant T_{HS}$, the warning distance is:

$$WD = 0.5(A_{Hmax} - A_L)T_M^2 + (A_H - A_{Hmax})PRT \cdot T_M - RR \cdot T_M - 0.5(A_H - A_{Hmax})PRT^2 + D_0 \quad (4)$$

The NHTSA algorithm contains three free parameters: the minimum distance between the leading vehicle and the host vehicle (D_0), the perception-reaction time of the subject driver (PRT), and the maximum deceleration of the host vehicle (A_{Hmax}). These parameters are candidate ADAS algorithm parameters to be optimized, because changing their levels can alter the timing when the ADAS starts to interact with the subject driver. In practice, D_0 is usually set to a constant equal to the average vehicle spacing in jam traffic (e.g., 2 m). The PRT of the subject driver changes from time to time as the driver interacts with ADAS. It is not proper to use it as the ADAS algorithm parameter for optimization. Based on the above discussion, the A_{Hmax} is taken as the second ADAS algorithm parameter to be optimized. The influence of A_{Hmax} on the warning distance is visualized by Fig. 2.

The existing studies adopt A_{Hmax} in a range between 0.1 g and 0.9 g ($g = 9.8$ m/s^2, gravity acceleration) (Brunson et al., 2002; Lee et al., 2002). A smaller A_{Hmax} would result in a longer warning distance and earlier collision warning, and a larger A_{Hmax} shorter warning distance and later collision warning. In this case, the boundary of the warning distance threshold s^*_{ADAS} is given as:

$$WD^*_{ADAS} = WD(A^*_{Hmax}), A^*_{Hmax} \in [0.1g, 0.9g] \quad (5)$$

3.2. Modeling driver behavior adaptation under the influence of ADAS

According to the existing studies as enlisted in Table 1, the FCW function of the ADAS primarily impact subject drivers' behavior regarding the PRT and DH. The headway adaptation arises because the ADAS continuous reminds the subject driver of her real-time headway via a color-based human machine interface (e.g., red icon means a lower than threshold headway and green icon means larger). In this case, the subject driver can easily maintain her headway in a safe and consistent level and the headway records are closely distributed around the headway threshold set by the ADAS.

When modeling drivers' headway adaptation, the uncertainty of a driver's compliance level to the ADAS information needs to be considered. To this end, a compliance index σ is assigned to each of the modeled drivers. The index is a random integer that ranges between 0 and 100. A driver with a compliance index of 0 completely ignores the information sent by the ADAS, whereas a driver with a compliance index of 100 completely follows the instructions given by the ADAS.

The ADAS does not interact with the equipped drivers all the time. It only becomes active when there are traffic events that require the drivers' attention. The ADAS stops the interaction when the events no longer exist. In this case, the impact of the ADAS on the driving behavior does not exist all the time. In this study, we assume that the influence of the ADAS reaches its maximum level as the ADAS triggers an alarm. The maximum influence will last for a short time, during which the driver's behavior parameters adapt to different levels. This period is referred to as the ADAS influence time. Afterwards, the influence of the ADAS will slowly decrease and finally disappear. The period of the influence decrease is called recovering time. The two time periods are visualized in Fig. 3.

After incorporating the uncertainty of the compliance level and the ADAS influence time, the ADAS-affected headway is mathematically given as:

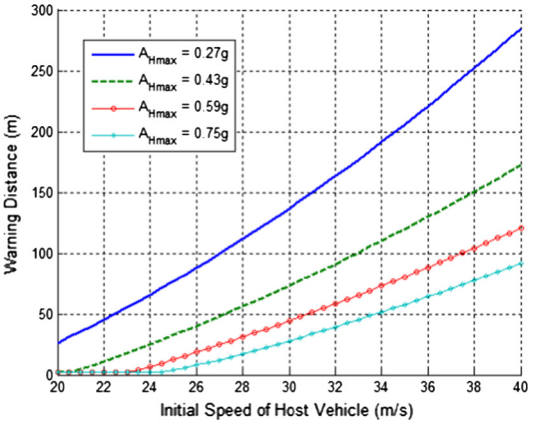

Parameters used in this plot: initial speed of the leading vehicle = 30 m/s; deceleration of the leading vehicle = -0.55g; PRT = 1.4 s; and D_0 = 2 m.

Fig. 2. Warning distance under various A_{Hmax} levels.

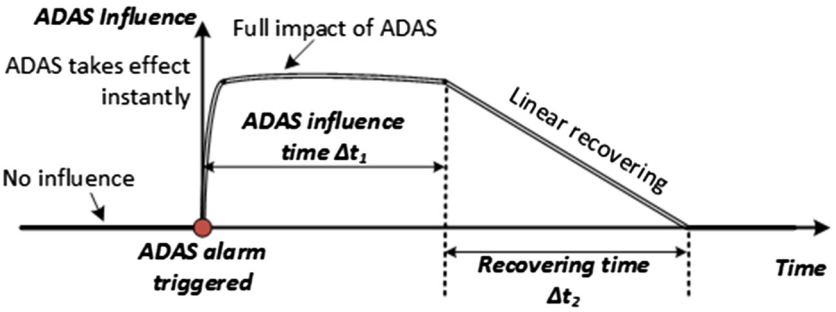

Fig. 3. Visualization of ADAS influence time and recovering time.

$$DH^* = \begin{cases} DH_1 = DH_0 + (HW_{ADAS} - DH_0) \cdot \frac{\sigma}{100} & t < \Delta t_1 \\ DH_2 = DH_1 + (DH_0 - DH_1) \cdot \frac{t - \Delta t_1}{\Delta t_2} & \Delta t_1 \leqslant t < \Delta t_1 + \Delta t_2 \\ DH_0 & \text{otherwise} \end{cases} \tag{6}$$

where t is the time elapsed since the ADAS triggers the alarm.

The PRT is defined as the time gap between the onset of a traffic event (such as the braking light of the leading vehicle is on) and the onset of the subject driver's response to the event. As stated by Treiber and Kesting (2013), the PRT contains the mental processing time, the movement or action time, and the technical response time of the vehicle. The mental processing time is the duration in which the driver assesses the traffic condition and decides proper actions to take. It is further divided into the sensation time, the perception time, the situation awareness time, and the decision time (see Fig. 4).

The PRT reduction is observed as the ADAS sends collision warnings. Before the warning is issued, the ADAS has completed the sensation, perception and situation recognition in the background via the wireless communication. The primary wireless communication technology of the ADAS is the Dedicated Short Range Communication (DSRC), which has a very small communication latency (e.g., in the order of 0.002 s, see Hill and Krueger, 2016). For this reason, the ADAS can perform situation recognition much faster than human drivers, and consequently help reduce the total time required by a driver in response to an event. In addition, upon receiving the message, the subject driver becomes aware of the imminence of a potential collision and understands where the risk comes from (i.e., from the leading vehicle). The Highway Safety Manual (AASHTO, 2010) reported that a human driver generally responds much faster to expected events than to unexpected events. When the ADAS is involved in the driver's decision-making process, the driver's PRT is defined as the summation of ADAS's communication and situation recognition time, the information processing time, the decision time, the movement time, and the technical response time, as shown by Fig. 4. The information processing time is the time period required by the driver to understand the ADAS information.

Table 1 reveals that the PRT reduction of an ADAS-equipped driver could be in a range of 10% to 50%. Similar to the DH model, the ADAS affected PRT is described as follows:

$$PRT^* = \begin{cases} PRT_1 = PRT_0(1 - 10\% - 40\% \cdot \frac{\sigma}{100}) & t < \Delta t_1 \\ PRT_2 = PRT_1 + (PRT_0 - PRT_1) \cdot \frac{t - \Delta t_1}{\Delta t_2} & \Delta t_1 \leqslant t < \Delta t_1 + \Delta t_2 \\ PRT_0 & \text{otherwise} \end{cases} \tag{7}$$

These ADAS-affected driving behaviors are incorporated into the Intelligent Driver Model (IDM, see Treiber et al., 2006). In the IDM, a driver's acceleration is modeled as a function of her own speed and the following distance. The desired following distance is a function of the driver's speed, desired headway, and the relative speed to the leading vehicle. In each update interval, the IDM computes the ratio between the speed and the driver's desired speed and the ratio between the following distance and the desired distance. If the ratios are less than 1, the driver tends to accelerate. The intensity of the acceleration is determined based on magnitude of the ratios. In this study, the IDM has been modified in the two aspects: (1) a delay term is added to represent the driver's perception reaction time; and (2) a desired headway function described by Eq. (6) is used to replace the constant desired headway adopted in the original IDM model. The modified IDM is mathematically represented by the following equations:

$$\dot{v}(t + PRT) = a\left[1 - \left(\frac{v(t + PRT)}{v_0}\right)^{\alpha} - \left(\frac{s^*(v(t + PRT), \Delta v(t))}{s(t)}\right)^{\beta}\right] \tag{8}$$

$$s^*(v, \Delta v) = s_0 + max\left(0, v \cdot DH + \frac{v\Delta v}{2\sqrt{ab}}\right) \tag{9}$$

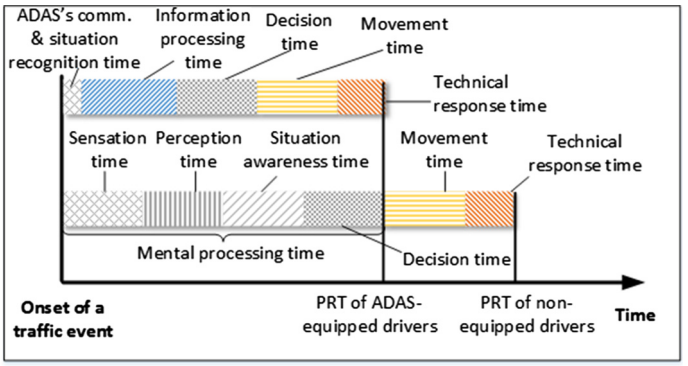

Fig. 4. Components of PRT.

In the presented methodology framework, the variation of the behavior parameters among drivers are considered by assigning normal distributed v_0, DH and PRT to individual drivers. After incorporating the PRT term into the IDM, the model will produce vehicle collisions. Nonetheless, realistic modeling of traffic accidents is beyond the capability of the modified IDM. Thus, these artificial collisions are removed from the numeric simulation algorithm. The assumption for the model simplification is that the drivers will brake strongly to prevent severe conflicts from developing into collisions. During the hard brake process, the drivers highly concentrate on the action in and their response is very fast manner. The assumption is implemented such that a modeled driver's response delay will be relaxed from Eq. (8) if the driver is about to collide with the leading vehicle in the next second. Once the response delay is removed, the subject driver will slow down immediately with a large deceleration. The potential collision can be avoided because of the large deceleration.

The lane-changing model developed by Hidas (2002, 2005) is used to capture the lateral movements of the modeled vehicles. In the Hidas model, a lane change may be considered 'desirable' or 'essential'. A driver feels 'desirable' to make a lane change if she tries to gain speed advantage in the target lane. On the other hand, a driver's lane-changing desire is 'essential' when the driver must perform a lane change in order to continue her or his route. Once a driver is motivated to perform a lane change, she will choose to perform either a free, cooperative, or forced maneuver. In a desirable lane change, the subject driver will only attempt to perform the free maneuver, which does not involve the interaction between the subject driver and the lag vehicle (see Fig. 5). In an essential lane change, the subject driver will first seek for the opportunity to make a free maneuver. If it is not possible, the driver will check if the lag vehicle is willing to courteously slow down and create a gap. If the lag vehicle starts to slow down, she will merge into the created gap and completes a cooperative maneuver. In case the subject driver is unable to conduct a free or cooperative maneuver, she will decide to force into the target lane, which results in a forced maneuver.

The modeled lane change behavior differs with the real lane change behavior in the following aspects. First, the lane change maneuver is assumed to take place instantly. In addition, the maximum deceleration accepted by drivers involved in a lane change is much larger than the maximum deceleration used in the normal car-following condition. Finally, the model does not consider the relaxation behavior, which describes the gradual increase of the following distance after the completion of a lane change. After applying the modeling assumptions, the traffic flow models are able to closely reproduce the traffic flow patterns observed at the study site.

In the methodology framework, the IDM and Hidas models are embedded into the Matlab environment. The models are executed through a Matlab script that outputs the vehicle location, speed and acceleration in each update interval. The outputs are then input into the VISSIM environment with external programming codes via the .COM interface. The trajectories of the modeled vehicles are visualized through running the rebuilt VISSIM model. The following table shows the pseudocode that depicts the programming algorithm executed at each simulation time step (see Table 5).

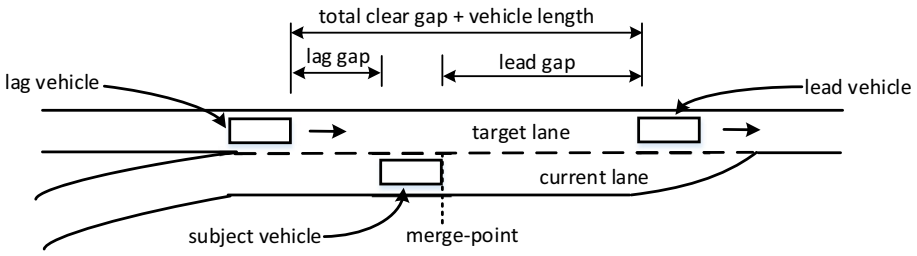

Fig. 5. Illustration of vehicles involved in a lane change.

Table 5
Algorithm for modeling behavior impact of ADAS.

```
DEFINE t = 0; (t represents time elapsed since the ADAS triggers alarm)
DH* = DH0;
PRT* = PRT0;
FOR each ADAS-equipped vehicle in the network
    IF actual headway < HW_ADAS AND actual spacing >= WD
      DH* = DH1;
      t = time step;
    ELSE IF actual headway ⩾ HW_ADAS AND actual spacing < WD
      PRT* = PRT1;
      t = time step;
    ELSE IF actual headway < HW_ADAS AND actual spacing < WD
      DH* = DH1;
      PRT* = PRT1;
      t = time step;
    ELSE
      IF 0 < t < Δt1
          DH* = DH1;
          PRT* = PRT1;
          t = t + time step;
      ELSE IF Δt1 < t < Δt1 + Δt2
          DH* = DH2;
          PRT* = PRT2;
          t = t + time step;
      ELSE
          DH* = DH0;
          PRT* = PRT0;
          t = 0;
      END IF
    END IF
END FOR
```

3.3. Identification of optimal ADAS algorithm parameter set

In this study, the Genetic Algorithm (GA) is adopted to search the optimal HW_{ADAS} and A_{Hmax} that enable the optimization safety and mobility MOEs. The GA iteratively executes the car-following and lane-changing models presented in Section 3.2 and computes the MOEs at various HW_{ADAS} and A_{Hmax} levels. The optimization programing can be expressed by the following equation:

$$\max \boldsymbol{M} \; S.T. \begin{cases} \boldsymbol{x} \in \boldsymbol{\Omega} \\ I_{ex} = I_{ex}^{*} \end{cases} \tag{10}$$

where $\boldsymbol{M}$ is a vector containing the target MOEs; $\boldsymbol{x} = \begin{bmatrix} HW_{ADAS} \\ A_{Hmax} \end{bmatrix}$; $\boldsymbol{\Omega} = \begin{bmatrix} HW_{ADAS}^{*} \\ A_{Hmax}^{*} \end{bmatrix}$; the constraint I_{ex}^{*} represents exogenous parameters (in comparison to endogenous parameters such as the driving behaviors) that affect dynamics of a traffic flow stream at a study highway facility. In the presented methodology, I_{ex} includes the highway facility type (e.g., basic freeway segment, freeway weaving/merging/diverging segment, arterial or intersection), traffic demand, fleet composition, and penetration rate of the ADAS. The optimal set of the ADAS parameters $\hat{\boldsymbol{x}}$ are found if for some neighborhood of $\hat{\boldsymbol{x}}$ there does not exist a $\Delta\boldsymbol{x}$ such that $\boldsymbol{x} + \Delta\boldsymbol{x} \in \boldsymbol{\Omega}$ and

$$\begin{aligned} &M_i(\hat{\boldsymbol{x}} + \Delta\boldsymbol{x}) \leqslant M_i(\hat{\boldsymbol{x}}), \forall i \text{ and} \\ &M_i(\hat{\boldsymbol{x}} + \Delta\boldsymbol{x}) < M_i(\hat{\boldsymbol{x}}) \text{ for at least one } i \end{aligned} \tag{11}$$

where $\hat{\boldsymbol{x}}$ might contain multiple points. While moving from one point to another, there is always a certain amount of sacrifice in one MOE to achieve a certain amount of gain in the other(s).

In this study, the safety MOE is the average number of conflicts experienced by a driver as she passes the concerned road segment. The occurrence of a conflict is identified by using the TTC measure. The TTC is defined as the time remaining until a collision will occur between two vehicles if their collision course and speed difference are maintained (Hayward, 1972). If at some time the TTC of a subject driver drops below a threshold TTC, it indicates the start of a conflict; and later as the TTC rises above the threshold again, the conflict is ended. The TTC is mathematically given:

$$TTC = \begin{cases} \frac{D}{v_S - v_L}, & v_L < v_S \\ \infty, & \text{otherwise} \end{cases} \tag{12}$$

where D is the spacing between the leading vehicle and the subject driver; v_L is the speed of the leading vehicle; and v_S is the speed of the subject driver. In this research, the threshold TTC is 1.5 s, as recommended by Gettman et al. (2008).

The mobility MOEs are the highway throughput in number of vehicles per hour per lane (veh/hr/ln) and the average travel delay reduction per vehicle (s/veh). The delay is computed as the difference between a driver's actual travel time through a road segment and the travel time the driver would have if she travels at the free flow speed of the road segment. It is computed by the following equation:

$$delay_i = t_i - S/v_0 \tag{13}$$

where t_i is the actual travel time of driver i; S is the length of the study site; and v_0 is the free flow speed.

4. Case study for a freeway bottleneck

4.1. Study site description

A freeway segment at northbound I-71 freeway close to Exit #12 in the Greater Cincinnati area, Ohio is taken as the study site in this research (see Fig. 6). The freeway mainline has three lanes. The Montgomery on-ramp is connected to the northbound freeway mainline by a 110-m acceleration. The on-ramp is 390 m in length. A five-weekday traffic data count was performed at this site in June 2015 to obtain the traffic demand data. The mean peak hour traffic volume of the freeway is found to be 4400 vehicles per hour, with 4.5% of heavy-duty vehicles. The mean peak hour ramp traffic is 950 vehicles per hour, with 1% of heavy-duty vehicles. This site has recurrent traffic congestions, mainly due to the traffic disturbances caused by the large ramp flow. In the case study, the traffic data is collected in a 900-m freeway segment that covers the on-ramp merging area. A 1600-m freeway segment upstream of the area is also included in the simulation study. This segment allows the modeled vehicles to fully interact before entering the data collection area.

4.2. Calibration and validation of traffic flow models

The calibration and validation of the IDM and Hidas model are carried out following the procedure developed by Park and Won (2006). The objective of the model calibration is that, given the peak hour traffic inputs, the calibrated models are able to reproduce key traffic flow parameters that are compatible with the real-world observations. The key traffic flow parameters used in the calibration are mean vehicle travel time over the 900-meter data collection segment (travel time) and mean vehicle speed at the beginning of the acceleration lane (entry speed). The benchmark travel time and entry speed are collected by using GPS-equipped floating cars from 2013 to 2016. The traffic data collected under the congested traffic conditions are used for the calibration and validation. A data point falls into the congested traffic condition if the travel time is larger than 50 s—our data inspection indicates that the travel time under the free flow and congested traffic condition breaks down around 50 s. 250 GPS trajectory samples are used for calibration and another 238 samples for validation. The GA is used to search for the optimal IDM and Hidas model parameters at which the distribution differences between the modeled and observed travel time and entry speed are minimized. The model calibration adopts the following multi-objective optimization model:

$$\min \boldsymbol{p} - \boldsymbol{Values}\ S.T. \begin{cases} \boldsymbol{P_{IDM}} \in \boldsymbol{\Omega_{IDM}} \\ \boldsymbol{P_{Hidas}} \in \boldsymbol{\Omega_{Hidas}} \end{cases} \tag{14}$$

where $\boldsymbol{P}$ represents the calibrated model parameters; $\boldsymbol{\Omega}$ contains the parameter upper and lower bounds; and $\boldsymbol{p} - \boldsymbol{Values}$ contains the p-values of the Kolmogorov-Smirnov (K-S) tests. Two K-S tests are performed for the travel time and entry speed separately. The less the p-value is, the closer the modeled and observed travel time (entry speed) are. The calibrated IDM and Hidas parameters and the optimal parameter levels are shown in Table 6. As shown by Fig. 7, the modeled results are very consistent with the validation dataset.

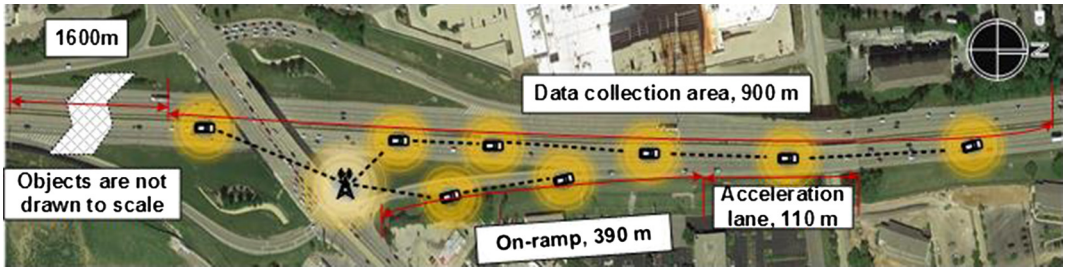

Fig. 6. Case study site.

Table 6
Calibrated traffic model parameters.

Model parameter	Optimal value
Maximum acceleration of cars a_{car}, m/s^2	1.1
Maximum acceleration of trucks a_{truck}, m/s^2	0.8
Maximum desirable deceleration of cars b_{car}, m/s^2	1.9
Maximum desirable deceleration of trucks b_{truck}, m/s^2	1.5
Minimum spacing s_0, m	2.0
Desired speed v_0, m/s	31.0
Standard deviation of v_0, m/s	2.0
Desired HW of non-ADAS equipped driver, s	1.2
Standard deviation of HW, m	0.2
PRT of non-ADAS equipped driver, s	1.2
Standard deviation of PRT, m	0.2
Coefficient α	4
Coefficient β	2
Maximum deceleration of subject driver in cooperative or forced lane changes, m/s^2	2.3
Maximum deceleration of lag vehicle in cooperative lane changes, m/s^2	2.3
Maximum deceleration of lag vehicle in forced lane changes, m/s^2	6.0

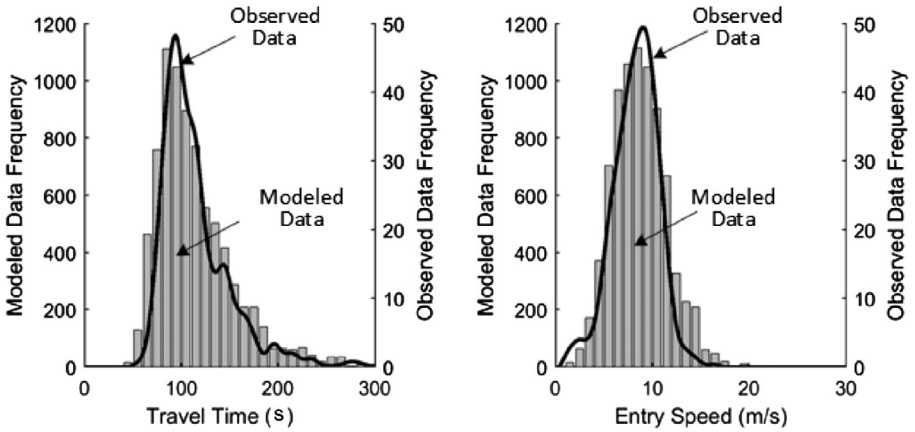

Fig. 7. Traffic model validation results.

4.3. Case study results and discussion

The case study considers a base scenario and three ADAS scenarios. In the base scenario, none of the modeled drivers are equipped with the ADAS. Results of the base scenario represent the existing traffic condition. The three ADAS scenarios incorporate low, medium and high ADAS marketing penetration rates, respectively. In each ADAS scenario, the modeled drivers are first assumed to randomly choose the HW_{ADAS} and A_{Hmax} levels. Their compliance level to the ADAS information is also a random variable that follows the normal distribution. Afterwards, the traffic management strategy is assumed to be implemented. In this case, the drivers will consistently adopt the HW_{ADAS} and A_{Hmax} level recommended by the traffic management team. Their compliance level will become higher and less dispersed. We perform 20 simulation runs for each scenario. The time period of each run is 90 min. The first 30 min are warm-up period. The data collected in the remaining 60 min is adopted for the scenario comparison. Parameters used to define the scenarios are listed in Table 7.

We first compare the MOEs among the base scenario and the ADAS scenarios in which drivers randomly choose HW_{ADAS} and A_{Hmax}. As Table 8 shows, the mean and standard deviation of the average conflicts measure decreases with the increase of the ADAS penetration rate—more conflicts can be avoided as greater number of drivers are assisted with the ADAS. Nonetheless, the magnitude of the safety improvement is too small under the medium and high penetration rate scenarios. For example, there is only 7.2% extra decrease of conflict as the penetration rate increases from 20% to 55%; and 4.3% extra decrease of conflict as the penetration rate grows from 55% to 90%. In addition, the mobility MOEs even become worse as the penetration rate increases. The reason for the throughput decrease is that the ADAS-equipped drivers tend to keep larger time headway than non-equipped drivers. As a result, the ADAS-equipped drivers will maintain longer following distance than non-equipped drivers under the same speed. The longer following distance leads to smaller vehicle density and smaller throughput. The larger delay is caused by the unique acceleration and deceleration patterns of the ADAS-equipped drivers. Before entering a congested region (e.g., a stop-and-go wave), a ADAS-equipped driver will begin decelerating at a larger distance than a non-equipped driver. After the ADAS-equipped driver passes the congested region, she will not start to accelerate

Table 7
Scenario parameters.

Parameter	Scenarios						
	Base	ADAS 1-1	ADAS 1-2	ADAS 2-1	ADAS 2-2	ADAS 3-1	ADAS 3-2
Penetration rate	0%	20%	20%	55%	55%	90%	90%
Mean compliance level	NA	50	90	50	90	50	90
Standard deviation of compliance level	NA	50	10	50	10	50	10
HW_{ADAS} lower bound	NA	1.2 s	1.2 s	1.2 s	1.2 s	1.2 s	1.2 s
HW_{ADAS} upper bound	NA	2.4 s	2.4 s	2.4 s	2.4 s	2.4 s	2.4 s
A_{Hmax} lower bound	NA	0.1 g	0.1 g	0.1 g	0.1 g	0.1 g	0.1 g
A_{Hmax} upper bound	NA	0.9 g	0.9 g	0.9 g	0.9 g	0.9 g	0.9 g
ADAS influence time	NA	5 s	5 s	5 s	5 s	5 s	5 s
Recovering time	NA	10 s	10 s	10 s	10 s	10 s	10 s

Table 8
Comparison among scenarios.

Scenario	Penetration rate	Delay (s/veh)		Throughput (veh/h/ln)		Conflict (1/veh)	
		Mean	Std	Mean	Std	Mean	Std
Base	0%	82.3	13.9	1305	26	2.7	0.5
ADAS 1-1	20%	74.6 (−9.4%)	13.3	1316 (+0.8%)	19	2.2 (−18.5%)	0.4
ADAS 2-1	55%	83.4 (+1.3%)	12.4	1316 (+0.8%)	26	2.0 (−25.9%)	0.3
ADAS 3-1	90%	106.9 (+29.9%)	15.4	1286 (−1.5%)	12	1.9 (−29.6%)	0.3

Std: standard deviation; changes comparing with the base scenario are shown by numbers in the parentheses.

until the headway to the leading vehicle is longer than her desired headway. Because of these behaviors, the ADAS-equipped drivers will end up with smaller average travel speed, and thus larger delay. The safety improvement is not significant, because the ADAS intensifies behavior heterogeneity among drivers by enlarging the behavior differences of the ADAS-equipped drivers and non-equipped drivers and changing the behavior of the ADAS-equipped driver changes from time to time. Such a heterogeneity gets even larger as the ADAS-equipped drivers are allowed to randomly setup the ADAS algorithm parameters. The behavior heterogeneity may negatively affect the traffic flow stability, and offset the safety benefit of the ADAS.

Previous discussion reveals that the implementation of the ADAS may not lead to the expected traffic mobility and safety improvement. One major reason is that the ADAS-equipped drivers randomly set up the ADAS parameter levels, resulting in increased heterogeneity among drivers. If the ADAS-equipped drivers can consistently accept a ADAS parameter level, the traffic mobility and safety performance might be improved comparing to the random parameter case. To test the hypothesis, we first conduct a preliminary analysis at finite HW_{ADAS} and A_{Hmax} levels. The considered HW_{ADAS} levels range from 1.2 s to 2.4 s, with 0.3 s increment; and the A_{Hmax} levels range from 0.1 g to 0.9 g, with 0.2 g increment. Thus 25 cases (5 HW_{ADAS} levels times 5 A_{Hmax} levels) have been considered in the preliminary analysis. The tested HW_{ADAS} and A_{Hmax} combinations cover the entire domain of the two parameters. If substantial mobility or safety improvement is identified at some combinations, it is worthy to continue the search for the optimal HW_{ADAS} and A_{Hmax} levels. Table 9 depicts the HW_{ADAS} and A_{Hmax} combinations

Table 9
Mobility and safety performance at finite HW_{ADAS} and A_{Hmax} levels.

Scenarios	HW_{ADAS} (s)	A_{Hmax} (m/s^2)	T_{ADAS}%	$\overline{PRT}$(s)	$\overline{HW}$(s)	Delay (s/veh)	Throughput (veh/h/ln)	Conflict (1/veh)
ADAS 1-1	Random	Random	9.2%	1.16	1.23	74.6	1316	2.2
ADAS 1-2	1.8	0.9 g	7.70%	1.16	1.22	73.6	1322	2.1
	1.8	0.7 g	7.90%	1.16	1.22	73.3	1320	2.1
ADAS 2-1	Random	Random	25.3%	1.12	1.30	83.4	1316	2.0
ADAS 2-2	1.8	0.9 g	20.7%	1.12	1.27	73.5	1321	1.6
	1.8	0.1 g	33.0%	1.05	1.27	80.9	1404	1.9
	1.5	0.7 g	20.2%	1.11	1.22	71.9	1366	1.9
	1.2	0.9 g	17.9%	1.11	1.20	69.2	1385	1.9
ADAS 3-1	Random	Random	41.5%	1.09	1.38	106.9	1286	1.9
ADAS 3-2	2.1	0.1 g	58.40%	0.95	1.43	105.1	1344	0.8
	1.8	0.9 g	34.20%	1.09	1.33	91.1	1322	1.8
	1.8	0.7 g	35.20%	1.09	1.33	96.5	1335	1.9
	1.8	0.1 g	54.80%	0.95	1.30	84.9	1477	1.2
	1.5	0.9 g	31.20%	1.07	1.23	75.4	1413	1.9
	1.5	0.1 g	51.50%	0.95	1.23	80.4	1538	1.5
	1.2	0.1 g	49.50%	0.96	1.20	71.7	1557	1.5

that incur improved mobility and safety MOEs. In addition, the percentage of the ADAS influence time over the total vehicle time traveled ($T_{ADAS}\%$), and the average PRT ($\overline{PRT}$) and desired headway ($\overline{HW}$) of the modeled drivers are listed in the table for better analysis. Based on these factors, we confirm that the ADAS interacts with drivers more frequently not only as the penetration rate increases, but also as the HW_{ADAS} increases or the A_{Hmax} decreases. Moreover, the average PRT and headway increase as the HW_{ADAS} and A_{Hmax} levels become higher.

Comparing to scenario 1-1, the improvement of the MOEs in scenario 1-2 is insignificant. Since the penetration rate of the ADAS is low in scenario 1, the overall traffic operation will not have much change even though all ADAS-equipped drivers behave consistently. It suggests that there is no much benefit to implement the traffic management under low ADAS penetration rate. On the other hand, larger number of HW_{ADAS} and A_{Hmax} combinations have led the improved MOEs in scenario 2 and 3. The MOE improvement is also very significant. Hence the optimal ADAS parameter search should be carried out for the medium and high ADAS penetration rate scenarios.

The optimal HW_{ADAS} and A_{Hmax} levels for scenario 2, and their corresponding MOEs are shown in Table 10. The optimal points are visualized in Fig. 8. The optimal performance is reached when the HW_{ADAS} is in the middle range (e.g., 1.6 s to 1.8 s) and the A_{Hmax} is in the high range (e.g., 0.8 g to 0.9 g). In this case, the ADAS encourages the subject drivers to keep a slightly longer headway than the non-equipped drivers. As the A_{Hmax} is set to a high level, the ADAS only triggers the collision alarm when very severer conflicts take place. Under the optimal HW_{ADAS} and A_{Hmax} levels, the conflict and delay measures have the most significant improvement. It indicates that the reduction of behavior heterogeneity among ADAS-equipped drivers can further take down the number of traffic conflicts. The reduction of conflicts leads to the decline of the traffic disturbances. Consequently, the ADAS-equipped drivers encounter fewer deceleration and acceleration cycles, resulting increase of the average travel speed and reduction of the delay. Nonetheless, the throughput improvement is not as prominent as the other two MOEs. This is because the desired average headway of the drivers gets bigger under the optimal HW_{ADAS} levels. The negative impact of the increased headway on the throughput can offset the mobility benefit brought by the ADAS.

The optimal HW_{ADAS} and A_{Hmax} levels for scenario 3, and their corresponding MOEs are shown in Table 11. The optimal points are visualized in Fig. 9. The optimal points are found at the lowest A_{Hmax} level (i.e., 0.1 g). In this case, the ADAS alarm

Table 10
Optimal HW_{ADAS} and A_{Hmax} levels for scenario 2.

Scenario	HW_{ADAS} (s)	A_{Hmax} (m/s^2)	Delay (s/veh)		Throughput (veh/h/ln)		Conflict (1/veh)	
			Mean	Std	Mean	Std	Mean	Std
ADAS 2-1	Random	Random	83.4	12.4	1316	26	2.0	0.3
ADAS 2-2	1.76	0.90 g	67.2 (−19.4%)	10.5	1333 (+1.3%)	19	1.76 (−12.0%)	0.3
	1.73	0.89 g	67.7 (−18.8%)	10.7	1341 (+1.9%)	29	1.73 (−13.5%)	0.4
	1.67	0.89 g	69.2 (−17.0%)	11.4	1353 (+2.8%)	13	1.67 (−18.5%)	0.4
	1.65	0.88 g	69.9 (−16.2%)	9.6	1356 (+3.0%)	18	1.65 (−16.5%)	0.3
	1.62	0.88 g	70.9 (−15.0%)	9.0	1360 (+3.3%)	17	1.62 (−19.0%)	0.3

Changes are shown by numbers in the parentheses.

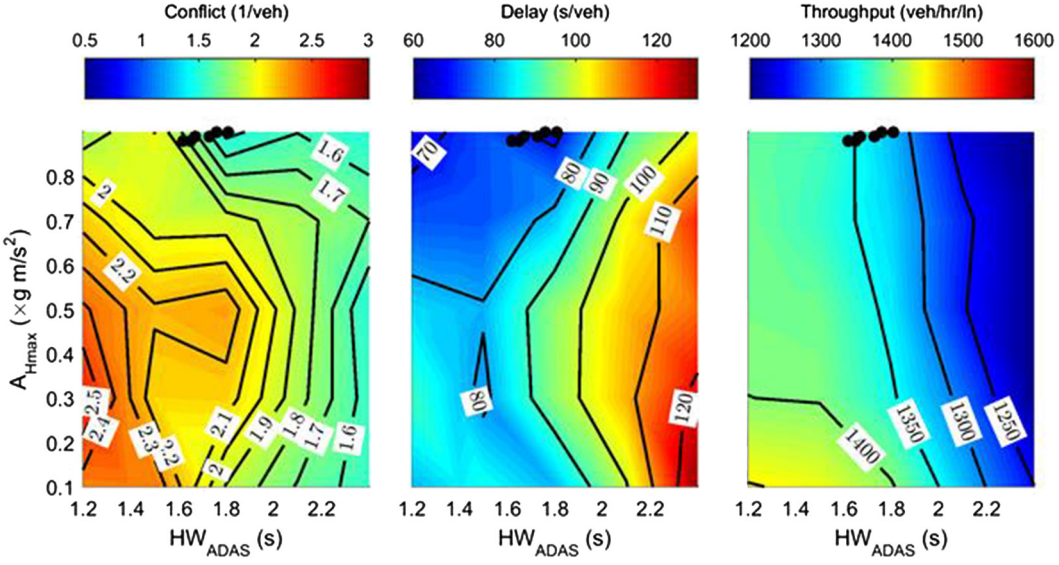

Fig. 8. Visualization of optimal HW_{ADAS} and A_{Hmax} levels for scenario 2.

Table 11
Optimal HW_{ADAS} and A_{Hmax} levels for scenario 3-2.

Scenario	HW_{ADAS} (s)	A_{Hmax} (m/s^2)	Delay (s/veh)		Throughput (veh/h/ln)		Conflict (1/veh)	
			Mean	Std	Mean	Std	Mean	Std
ADAS 3-1	Random	Random	106.9	15.4	1286	12	1.9	0.3
ADAS 3-2	2.1	0.1 g	102.3 (−4.3%)	7.0	1357 (+5.5%)	19	0.8 (−57.9%)	0.1
	2.0	0.1 g	97.1 (−9.2%)	10.7	1396 (+8.6%)	30	0.9 (−52.6%)	0.2
	1.9	0.1 g	93.7 (−12.3%)	9.3	1426 (+10.9%)	19	1.0 (−47.4%)	0.3
	1.8	0.1 g	87.5 (−18.1%)	8.2	1477 (+14.9%)	23	1.2 (−36.8%)	0.4
	1.6	0.1 g	79.8 (−25.4%)	9.8	1524 (+18.5%)	14	1.4 (−26.3%)	0.4
	1.2	0.1 g	74.0 (−30.8%)	8.8	1564 (+21.6%)	17	1.5 (−21.1%)	0.2

Changes are shown by numbers in the parentheses.

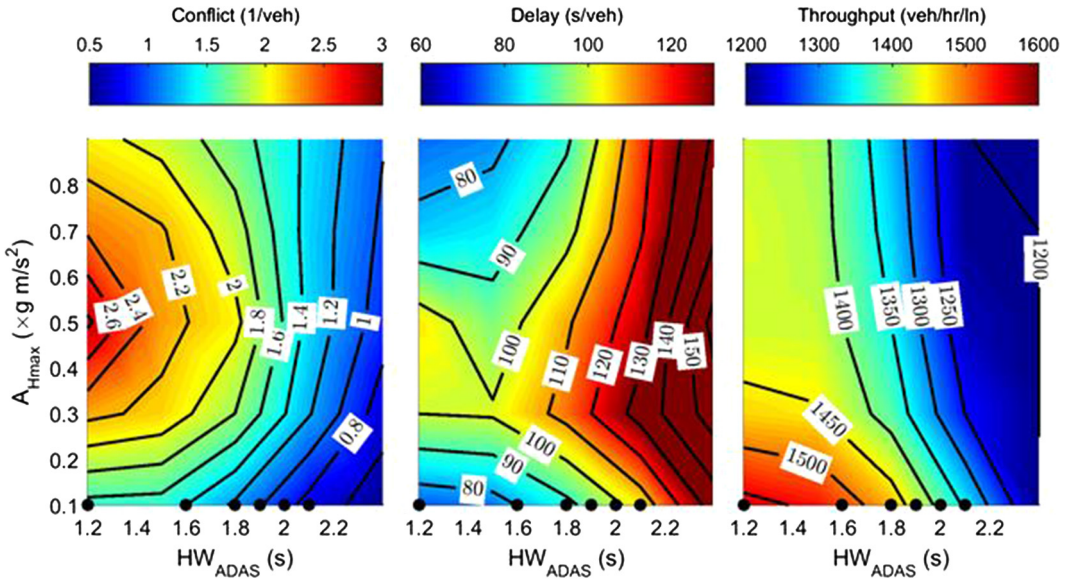

Fig. 9. Visualization of optimal HW_{ADAS} and A_{Hmax} levels for scenario 3.

will be triggered even if the conflict is a minor one. As a result, the system will interact with the subject drivers very frequently. On the other hand, the optimal HW_{ADAS} ranges from 1.2 s to 2.1 s. If the HW_{ADAS} is set to low levels (e.g., 1.2 s to 1.6 s), the mobility performance will be most significantly improved; if the HW_{ADAS} is set to high levels (e.g., 1.6 s to 2.1 s), the safety performance will have larger improvement than the mobility measures. The actual HW_{ADAS} for a concerned site can be determined based on the control priority of the specific site. For example, if recurrent congestions are observed at the site, the improvement of traffic efficiency might need to be prioritized. Thus the headway threshold should be set at lower levels so that the mobility MOEs can reach the optimal levels. On the other hand, if the primary objective is to improve the safety, the headway should be set at higher levels such that the number of conflicts are minimized. Comparing to the scenario 2, the optimal points are much more scattered in this scenario. It means that the optimal traffic operation can be achieved in greater HW_{ADAS} and A_{Hmax} ranges. In other words, the condition for optimization becomes less strict. In addition, both the throughput and conflict measures have much greater improvement in this scenario. The delay measure is worse than that of scenario 2 when the HW_{ADAS} is set to high levels, because in this case, the HW_{ADAS} is much larger than the optimal HW_{ADAS} of scenario 2. As discussed earlier, a larger headway can result in a smaller average travel speed and longer delay.

Results in Figs. 8 and 9 show that the change of MOEs is more rapid along the HW_{ADAS} axis than along the A_{Hmax} axis. It suggests that the HW_{ADAS} plays a more important role in influencing the MOEs than the A_{Hmax}. Since the ADAS continuously monitor the headway of a subject driver, the effect of HW_{ADAS} is cast on the subject driver all the time. On the other hand, the effect of A_{Hmax} only arises when the following distance is less than the warning distance. As the chance for a driver being affected by HW_{ADAS} is larger, the HW_{ADAS} terms play more significant role. Fig. 8 also suggests that the low HW_{ADAS} and A_{Hmax} levels (e.g., $HW_{ADAS} < 1.4s$ and $A_{Hmax} < 0.4g$) should be avoided when the ADAS penetration rate is 55%. At these HW_{ADAS} and A_{Hmax} levels, the ADAS makes the drivers overly sensitive to the traffic conflicts. Such a behavior of a ADAS-equipped driver might induce a chain of traffic conflicts to the following drivers, especially when the following drivers

are non-equipped drivers. The high HW_{ADAS} levels should also be avoided, because it causes drastic decrease of the mobility measures. Such a low traffic flow efficiency is not acceptable for a freeway facility. For scenario 3, the low HW_{ADAS} and median A_{Hmax} levels (e.g., $HW_{ADAS} < 1.4s$ and $0.4g < A_{Hmax} < 0.6g$) should be avoided (see Fig. 8). In these ranges, the traffic operation is most unstable and the largest number of conflicts per vehicle is observed.

5. Conclusion

Through a case study by using the proposed methodology, this research reveals that, if the ADAS-drivers set up the ADAS algorithm parameters freely, the implementation of the ADAS actually enlarges the behavior heterogeneity between the ADAS-equipped drivers and the non-equipped drivers. As a result, the systematic safety benefit of the ADAS becomes insignificant and the mobility performance even decreases as more ADAS-equipped vehicles emerge in the vehicle fleet. On the other hand, the study identifies the existence of optimal ADAS algorithm parameters HW_{ADAS} and A_{Hmax}, which are responsible for drivers' desired headway and PRT adaptation, respectively. If the optimal parameters are consistently accepted by drivers, the safety performance measured by the number of conflicts per vehicle and the mobility performance measured by average delay and highway throughput can be improved at the same time. Another interesting finding is that the level of traffic control required to achieve the optimal traffic mobility and safety performance increases as the ADAS penetration rate increases. Under the low penetration rate scenario, there is no need to ask the drivers to consistently implement the optimal ADAS algorithm parameters. In the medium and high penetration rate scenarios, it is preferable for the ADAS-equipped drivers to use the optimal ADAS algorithm parameters. Moreover, under the high ADAS penetration rate scenario, the optimal ADAS algorithm parameter set contains multiple distinct points, which offer alternative candidates for the traffic management centers as they develop traffic control strategies. For example, some optimal points correspond to the maximum safety MOE and suboptimal mobility MOEs while other points correspond to the maximum mobility MOEs and suboptimal safety MOE. These points can be easily applied for different control priorities (e.g., safety improvement first vs. mobility improvement first). Finally, the presented methodology is not exclusive to the FCW function evaluated in this study. It actually an open framework that is capable of incorporating other ADAS functions or other advanced transportation technologies, as long as their impact on driving behavior adaptation is quantified. Results from the framework are expected to lay out a solid foundation to further (1) promote successful deployment of the advanced technologies into the existing highway transportation systems; (2) facilitate the development new traffic information services in the traffic environment where the advanced technologies are deployed; and (3) enhance user experience in the traffic environment by offering them useful driving assistance information and driving behavior guidelines.

In our current research, some aspects of the behavior adaptation for both ADAS-equipped drivers and non-equipped drivers are not incorporated into presented methodology. For example, an ADAS-equipped driver might react differently to the same ADAS warning or advisory message due to the effect of the roadway environment and her mental state. After using the ADAS for a long period of time, the driver's behavior patterns may become different with the patterns observed as she first adopts the system. In addition, the non-equipped driver might have different reactions when interacting with ADAS-equipped drivers and non-equipped drivers. In the future, we will analyze these behavior aspects based on the reported empirical data and incorporate them into the presented methodology framework. In addition, the cognitive model describing human drivers' decision process will be integrated to more accurately predict the drivers' driving activities under the influence of the ADAS.

Acknowledgement

The authors appreciate the support of the U.S. Environmental Protection Agency via funded research through its Office of Research and Development. It has been subjected to the Agency's administrative review and has been approved for external publication. Any opinions expressed in this paper are those of the author(s) and do not necessarily reflect the views of the Agency; therefore, no official endorsement should be inferred. Any mention of trade names or commercial products does not constitute endorsement or recommendation for use.

References

Abe, G., Richardson, J., 2006. Alarm timing, trust and driver expectation for forward collision warning systems. Appl. Ergon. 37 (5), 577–586.
Adell, E., Várhelyi, A., dalla Fontana, M., 2011. The effects of a driver assistance system for safe speed and safe distance–a real-life field study. Transport. Res. Part C: Emerg. Technol. 19 (1), 145–155.
American association of state highway and transportation officials (AASHTO), 2010. Highway Safety Manual. AASHTO, Washington, D.C..
Ararat, Ö., Kural, E., & Güvenç, B. A. (2006). Development of a collision warning system for adaptive cruise control vehicles using a comparison analysis of recent algorithms. In: Intelligent Vehicles Symposium, 2006 IEEE. IEEE, pp. 194–199.
Aust, M.L., Engström, J., Viström, M., 2013. Effects of forward collision warning and repeated event exposure on emergency braking. Transport. Res. Part F: Traffic Psychol. Behav. 18, 34–46.
Bella, F., Russo, R., 2011. A Collision Warning System for rear-end collision: a driving simulator study. Procedia-Soc. Behav. Sci. 20, 676–686.
Bengler, K., Dietmayer, K., Farber, B., Maurer, M., Stiller, C., Winner, H., 2014. Three decades of driver assistance systems: Review and future perspectives. Intell. Transport. Syst. Magaz., IEEE 6 (4), 6–22.
Ben-Yaacov, A., Maltz, M., Shinar, D., 2002. Effects of an in-vehicle collision avoidance warning system on short-and long-term driving performance. Human Fact.: J. Human Fact. Ergon. Soc. 44 (2), 335–342.

Birrell, S.A., Fowkes, M., Jennings, P.A., 2014. Effect of using an in-vehicle smart driving aid on real-world driver performance. Intell. Transport. Syst., IEEE Transact. 15 (4), 1801–1810.
Brunson, S.J., Kyle, E.M., Phamdo, N.C., Preziotti, G.R., 2002. Alert Algorithm Development Program: NHTSA Rear-end collision Alert Algorithm (No. HS-809 526).
Bueno, M., Fabrigoule, C., Ndiaye, D., Fort, A., 2014. Behavioural adaptation and effectiveness of a Forward Collision Warning System depending on a secondary cognitive task. Transport. Res. Part F: Traffic Psychol. Behav. 24, 158–168.
Coelingh, E., Eidehall, A., Bengtsson, M., 2010. Collision warning with full auto brake and pedestrian detection-a practical example of automatic emergency braking. In: Intelligent Transportation Systems (ITSC), 2010 13th International IEEE Conference on. IEEE, pp. 155–160.
Farah, H., Koutsopoulos, H.N., Saifuzzaman, M., Kölbl, R., Fuchs, S., Bankosegger, D., 2012. Evaluation of the effect of cooperative infrastructure-to-vehicle systems on driver behavior. Transport. Res. Part C: Emerg. Technol. 21 (1), 42–56.
Farah, H., Koutsopoulos, H.N., 2014. Do cooperative systems make drivers' car-following behavior safer? Transport. Res. Part C: Emerg. Technol. 41, 61–72.
Gettman, D., Pu, L., Sayed, T., Shelby, S., 2008. Surrogate Safety Assessment Model and Validation. Report No. FHWA-HRT-08-051.
Hayward, J.C., 1972. Near-miss determination through use of a scale of danger. Highway Research Record, pp. 384.
Hegeman, G., Tapani, A., Hoogendoorn, S., 2009. Overtaking assistant assessment using traffic simulation. Transport. Res. Part C: Emerg. Technol. 17 (6), 617–630.
Hidas, P., 2002. Modelling lane changing and merging in microscopic traffic simulation. Transport. Res. Part C: Emerg. Technol. 10 (5), 351–371.
Hidas, P., 2005. Modelling vehicle interactions in microscopic simulation of merging and weaving. Transport. Res. Part C: Emerg. Technol. 13 (1), 37–62.
Hill, C., Krueger, G., 2016. ITS ePrimer, Module 13: Connected Vehicles. Accessible at <https://www.pcb.its.dot.gov/eprimer/module13.aspx>.
ISO 15623, 2002. Transport information and control systems – Forward Vehicle Collision Warning Systems – Performance Requirements and Test Procedures.
Jamson, A.H., Lai, F.C., Carsten, O.M., 2008. Potential benefits of an adaptive forward collision warning system. Transport. Res. Part C: Emerg. Technol. 16 (4), 471–484.
Jones, S., 2013. Cooperative Adaptive Cruise Control: Human Factors Analysis (No. FHWA-HRT-13-045).
Kesting, A., Treiber, M., Helbing, D., 2010. Enhanced intelligent driver model to access the impact of driving strategies on traffic capacity. Philosoph. Transact. Roy. Soc. Lond. A: Math., Phys. Eng. Sci. 368 (1928), 4585–4605.
Khondaker, B., Kattan, L., 2015. Variable speed limit: a microscopic analysis in a connected vehicle environment. Transport. Res. Part C: Emerg. Technol. 58, 146–159.
Kiefer R.J., Cassar M.T., Flannagan C.A., LeBlanc D.J., Palmer M.D., Deering R.K., Shulman M.A., 2003. Forward Collision Warning Requirements Project: Refining the CAMP Crash Alert Timing Approach by Examining "Last-Second" Braking and Lane Change Maneuvers Under Various Kinematic Conditions. (Report No. DOT-HS-809-574).
Koustanaï, A., Cavallo, V., Delhomme, P., Mas, A., 2012. Simulator training with a forward collision warning system effects on driver-system interactions and driver trust. Human Fact.: J. Human Fact. Ergon. Soc. 54 (5), 709–721.
Lee, J.D., McGehee, D.V., Brown, T.L., Reyes, M.L., 2002. Collision warning timing, driver distraction, and driver response to imminent rear-end collisions in a high-fidelity driving simulator. Human Fact.: J. Human Fact. Ergon. Soc. 44 (2), 314–334.
Lundgren, J., Tapani, A., 2006. Evaluation of safety effects of driver assistance systems through traffic simulation. Transport. Res. Rec.: J. Transport. Res. Board 1953, 81–88.
McGehee, D., Brown, T., Lee, J., Wilson, T., 2002. Effect of warning timing on collision avoidance behavior in a stationary lead vehicle scenario. Transport. Res. Rec.: J. Transport. Res. Board 1803, 1–6.
Miettinen, K., 2012. Nonlinear Multiobjective Optimization, vol. 12. Springer Science & Business Media.
Mohebbi, R., Gray, R., Tan, H.Z., 2009. Driver reaction time to tactile and auditory rear-end collision warnings while talking on a cell phone. Human Fact.: J. Human Fact. Ergon. Soc. 51 (1), 102–110.
Mulder, M., Kitazaki, S., Hijikata, S., Mulder, M., van Paassen, M.M., Boer, E.R., 2004, October. Reaction-time task during car-following with an active gas pedal. In Systems, Man and Cybernetics, 2004 IEEE International Conference on. IEEE, vol. 3, pp. 2465–2470.
Nodine, E., Lam, A., Stevens, S., Razo, M., Najm, W., 2011. Integrated vehicle-based safety systems (IVBSS) light vehicle field operational test independent evaluation (No. HS-811 516).
Park, B.B., Won, J., 2006. Microscopic Simulation Model Calibration and Validation Handbook (No. FHWA/VTRC 07-CR6).
Schakel, W.J., van Arem, B., Netten, B.D., 2010, September. Effects of cooperative adaptive cruise control on traffic flow stability. In: Intelligent Transportation Systems (ITSC), 2010 13th International IEEE Conference on. IEEE, pp. 759–764.
Shinar, D., Schechtman, E., 2002. Headway feedback improves intervehicular distance: a field study. Human Fact.: J. Human Fact. Ergon. Soc. 44 (3), 474–481.
Shladover, S., Su, D., Lu, X.Y., 2012. Impacts of cooperative adaptive cruise control on freeway traffic flow. Transport. Res. Rec.: J. Transport. Res. Board 2324, 63–70.
The U.S. Department of Transportation's National Highway Traffic Safety Administration (NHTSA), 2015. Advancing Safety on American's Roads. Accessible at <http://www.nhtsa.gov/nhtsa/accomplishments/2015/index.html> (retrieved 2015-12-10).
Treiber, M., Kesting, A., Helbing, D., 2006. Delays, inaccuracies and anticipation in microscopic traffic models. Phys. A: Stat. Mech. Appl. 360 (1), 71–88.
Treiber, M., Kesting, A., 2013. Traffic flow dynamics. Traffic Flow Dynamics: Data, Models and Simulation. Springer-Verlag, Berlin, Heidelberg.
Várhelyi, A., Kaufmann, C., Persson, A., 2015. User-related assessment of a Driver Assistance System for Continuous Support–a field trial. Transport. Res. Part F: Traffic Psychol. Behav. 30, 128–144.
Van Arem, B., Van Driel, C.J., Visser, R., 2006. The impact of cooperative adaptive cruise control on traffic-flow characteristics. IEEE Trans. Intell. Transp. Syst. 7 (4), 429–436.
Wang, M., Daamen, W., Hoogendoorn, S., Van Arem, B., 2014. Potential impacts of ecological adaptive cruise control systems on traffic and environment. IET Intel. Transport Syst. 8 (2), 77–86.